Physics Letters B 718 (2013) 1314–1320

Contents lists available at SciVerse ScienceDirect

Physics Letters B

www.elsevier.com/locate/physletb

Measurement of the $p\bar{p} \to W + b + X$ production cross section at $\sqrt{s} = 1.96$ TeV

D0 Collaboration

V.M. Abazov [af], B. Abbott [bp], B.S. Acharya [z], M. Adams [at], T. Adams [ar], G.D. Alexeev [af], G. Alkhazov [aj], A. Alton [be,1], A. Askew [ar], S. Atkins [bc], K. Augsten [g], C. Avila [e], F. Badaud [j], L. Bagby [as], B. Baldin [as], D.V. Bandurin [ar], S. Banerjee [z], E. Barberis [bd], P. Baringer [ba], J.F. Bartlett [as], U. Bassler [o], V. Bazterra [at], A. Bean [ba], M. Begalli [b], L. Bellantoni [as], S.B. Beri [x], G. Bernardi [n], R. Bernhard [s], I. Bertram [am], M. Besançon [o], R. Beuselinck [an], P.C. Bhat [as], S. Bhatia [bg], V. Bhatnagar [x], G. Blazey [au], S. Blessing [ar], K. Bloom [bh], A. Boehnlein [as], D. Boline [bm], E.E. Boos [ah], G. Borissov [am], A. Brandt [bs], O. Brandt [t], R. Brock [bf], A. Bross [as], D. Brown [n], J. Brown [n], X.B. Bu [as], M. Buehler [as], V. Buescher [u], V. Bunichev [ah], S. Burdin [am,2], C.P. Buszello [al], E. Camacho-Pérez [ac], B.C.K. Casey [as], H. Castilla-Valdez [ac], S. Caughron [bf], S. Chakrabarti [bm], D. Chakraborty [au], K.M. Chan [ay], A. Chandra [bu], E. Chapon [o], G. Chen [ba], S. Chevalier-Théry [o], S.W. Cho [ab], S. Choi [ab], B. Choudhary [y], S. Cihangir [as], D. Claes [bh], J. Clutter [ba], M. Cooke [as], W.E. Cooper [as], M. Corcoran [bu], F. Couderc [o], M.-C. Cousinou [l], A. Croc [o], D. Cutts [br], A. Das [ap], G. Davies [an], S.J. de Jong [ad,ae], E. De La Cruz-Burelo [ac], F. Déliot [o], R. Demina [bl], D. Denisov [as], S.P. Denisov [ai], S. Desai [as], C. Deterre [o], K. DeVaughan [bh], H.T. Diehl [as], M. Diesburg [as], P.F. Ding [ao], A. Dominguez [bh], A. Dubey [y], L.V. Dudko [ah], D. Duggan [bi], A. Duperrin [l], S. Dutt [x], A. Dyshkant [au], M. Eads [bh], D. Edmunds [bf], J. Ellison [aq], V.D. Elvira [as], Y. Enari [n], H. Evans [aw], A. Evdokimov [bn], V.N. Evdokimov [ai], G. Facini [bd], L. Feng [au], T. Ferbel [bl], F. Fiedler [u], F. Filthaut [ad,ae], W. Fisher [bf], H.E. Fisk [as], M. Fortner [au], H. Fox [am], S. Fuess [as], A. Garcia-Bellido [bl], J.A. García-González [ac], G.A. García-Guerra [ac,3], V. Gavrilov [ag], P. Gay [j], W. Geng [l,bf], D. Gerbaudo [bj], C.E. Gerber [at], Y. Gershtein [bi], G. Ginther [as,bl], G. Golovanov [af], A. Goussiou [bw], P.D. Grannis [bm], S. Greder [p], H. Greenlee [as], G. Grenier [q], Ph. Gris [j], J.-F. Grivaz [m], A. Grohsjean [o,4], S. Grünendahl [as], M.W. Grünewald [aa], T. Guillemin [m], G. Gutierrez [as], P. Gutierrez [bp], J. Haley [bd], L. Han [d], K. Harder [ao], A. Harel [bl], J.M. Hauptman [az], J. Hays [an], T. Head [ao], T. Hebbeker [r], D. Hedin [au], H. Hegab [bq], A.P. Heinson [aq], U. Heintz [br], C. Hensel [t], I. Heredia-De La Cruz [ac], K. Herner [be], G. Hesketh [ao,6], M.D. Hildreth [ay], R. Hirosky [bv], T. Hoang [ar], J.D. Hobbs [bm], B. Hoeneisen [i], J. Hogan [bu], M. Hohlfeld [u], I. Howley [bs], Z. Hubacek [g,o], V. Hynek [g], I. Iashvili [bk], Y. Ilchenko [bt], R. Illingworth [as], A.S. Ito [as], S. Jabeen [br], M. Jaffré [m], A. Jayasinghe [bp], M.S. Jeong [ab], R. Jesik [an], P. Jiang [d], K. Johns [ap], E. Johnson [bf], M. Johnson [as], A. Jonckheere [as], P. Jonsson [an], J. Joshi [aq], A.W. Jung [as], A. Juste [ak], E. Kajfasz [l], D. Karmanov [ah], P.A. Kasper [as], I. Katsanos [bh], R. Kehoe [bt], S. Kermiche [l], N. Khalatyan [as], A. Khanov [bq], A. Kharchilava [bk], Y.N. Kharzheev [af], I. Kiselevich [ag], J.M. Kohli [x], A.V. Kozelov [ai], J. Kraus [bg], A. Kumar [bk], A. Kupco [h], T. Kurča [q], V.A. Kuzmin [ah], S. Lammers [aw], G. Landsberg [br], P. Lebrun [q], H.S. Lee [ab], S.W. Lee [az], W.M. Lee [as], X. Lei [ap], J. Lellouch [n], D. Li [n], H. Li [k], L. Li [aq], Q.Z. Li [as], J.K. Lim [ab], D. Lincoln [as], J. Linnemann [bf], V.V. Lipaev [ai], R. Lipton [as], H. Liu [bt], Y. Liu [d], A. Lobodenko [aj], M. Lokajicek [h], R. Lopes de Sa [bm], H.J. Lubatti [bw], R. Luna-Garcia [ac,7], A.L. Lyon [as], A.K.A. Maciel [a], R. Madar [s], R. Magaña-Villalba [ac], S. Malik [bh], V.L. Malyshev [af], Y. Maravin [bb], J. Martínez-Ortega [ac], R. McCarthy [bm], C.L. McGivern [ao], M.M. Meijer [ad,ae], A. Melnitchouk [as], D. Menezes [au], P.G. Mercadante [c], M. Merkin [ah], A. Meyer [r], J. Meyer [t], F. Miconi [p], N.K. Mondal [z], M. Mulhearn [bv], E. Nagy [l], M. Naimuddin [y], M. Narain [br], R. Nayyar [ap], H.A. Neal [be], J.P. Negret [e], P. Neustroev [aj], H.T. Nguyen [bv], T. Nunnemann [v], J. Orduna [bu], N. Osman [l], J. Osta [ay], M. Padilla [aq], A. Pal [bs], N. Parashar [ax], V. Parihar [br], S.K. Park [ab], R. Partridge [br,5], N. Parua [aw], A. Patwa [bn], B. Penning [as], M. Perfilov [ah], Y. Peters [t], K. Petridis [ao], G. Petrillo [bl], P. Pétroff [m], M.-A. Pleier [bn],

0370-2693 Published by Elsevier B.V.
http://dx.doi.org/10.1016/j.physletb.2012.12.044

P.L.M. Podesta-Lerma [ac,8], V.M. Podstavkov [as], A.V. Popov [ai], M. Prewitt [bu], D. Price [aw], N. Prokopenko [ai], J. Qian [be], A. Quadt [t], B. Quinn [bg], M.S. Rangel [a], K. Ranjan [y], P.N. Ratoff [am], I. Razumov [ai], P. Renkel [bt], I. Ripp-Baudot [p], F. Rizatdinova [bq], M. Rominsky [as], A. Ross [am], C. Royon [o], P. Rubinov [as], R. Ruchti [ay], G. Sajot [k], P. Salcido [au], A. Sánchez-Hernández [ac], M.P. Sanders [v], A.S. Santos [a,9], G. Savage [as], L. Sawyer [bc], T. Scanlon [an], R.D. Schamberger [bm], Y. Scheglov [aj], H. Schellman [av], C. Schwanenberger [ao], R. Schwienhorst [bf], J. Sekaric [ba], H. Severini [bp], E. Shabalina [t], V. Shary [o], S. Shaw [bf], A.A. Shchukin [ai], R.K. Shivpuri [y], V. Simak [g], P. Skubic [bp], P. Slattery [bl], D. Smirnov [ay], K.J. Smith [bk], G.R. Snow [bh], J. Snow [bo], S. Snyder [bn], S. Söldner-Rembold [ao], L. Sonnenschein [r], K. Soustruznik [f], J. Stark [k], D.A. Stoyanova [ai], M. Strauss [bp], L. Suter [ao], P. Svoisky [bp], M. Titov [o], V.V. Tokmenin [af], Y.-T. Tsai [bl], K. Tschann-Grimm [bm], D. Tsybychev [bm], B. Tuchming [o], C. Tully [bj], L. Uvarov [aj], S. Uvarov [aj], S. Uzunyan [au], R. Van Kooten [aw], W.M. van Leeuwen [ad], N. Varelas [at], E.W. Varnes [ap], I.A. Vasilyev [ai], P. Verdier [q], A.Y. Verkheev [af], L.S. Vertogradov [af], M. Verzocchi [as], M. Vesterinen [ao], D. Vilanova [o], P. Vokac [g], H.D. Wahl [ar], M.H.L.S. Wang [as], J. Warchol [ay], G. Watts [bw], M. Wayne [ay], J. Weichert [u], L. Welty-Rieger [av], A. White [bs], D. Wicke [w], M.R.J. Williams [am], G.W. Wilson [ba], M. Wobisch [bc], D.R. Wood [bd], T.R. Wyatt [ao], Y. Xie [as], R. Yamada [as], S. Yang [d], T. Yasuda [as], Y.A. Yatsunenko [af], W. Ye [bm], Z. Ye [as], H. Yin [as], K. Yip [bn], S.W. Youn [as], J.M. Yu [be], J. Zennamo [bk], T. Zhao [bw], T.G. Zhao [ao], B. Zhou [be], J. Zhu [be], M. Zielinski [bl], D. Zieminska [aw], L. Zivkovic [br]

[a] *LAFEX, Centro Brasileiro de Pesquisas Físicas, Rio de Janeiro, Brazil*
[b] *Universidade do Estado do Rio de Janeiro, Rio de Janeiro, Brazil*
[c] *Universidade Federal do ABC, Santo André, Brazil*
[d] *University of Science and Technology of China, Hefei, People's Republic of China*
[e] *Universidad de los Andes, Bogotá, Colombia*
[f] *Charles University, Faculty of Mathematics and Physics, Center for Particle Physics, Prague, Czech Republic*
[g] *Czech Technical University in Prague, Prague, Czech Republic*
[h] *Center for Particle Physics, Institute of Physics, Academy of Sciences of the Czech Republic, Prague, Czech Republic*
[i] *Universidad San Francisco de Quito, Quito, Ecuador*
[j] *LPC, Université Blaise Pascal, CNRS/IN2P3, Clermont, France*
[k] *LPSC, Université Joseph Fourier Grenoble 1, CNRS/IN2P3, Institut National Polytechnique de Grenoble, Grenoble, France*
[l] *CPPM, Aix-Marseille Université, CNRS/IN2P3, Marseille, France*
[m] *LAL, Université Paris-Sud, CNRS/IN2P3, Orsay, France*
[n] *LPNHE, Universités Paris VI and VII, CNRS/IN2P3, Paris, France*
[o] *CEA, Irfu, SPP, Saclay, France*
[p] *IPHC, Université de Strasbourg, CNRS/IN2P3, Strasbourg, France*
[q] *IPNL, Université Lyon 1, CNRS/IN2P3, Villeurbanne, France and Université de Lyon, Lyon, France*
[r] *III. Physikalisches Institut A, RWTH Aachen University, Aachen, Germany*
[s] *Physikalisches Institut, Universität Freiburg, Freiburg, Germany*
[t] *II. Physikalisches Institut, Georg-August-Universität Göttingen, Göttingen, Germany*
[u] *Institut für Physik, Universität Mainz, Mainz, Germany*
[v] *Ludwig-Maximilians-Universität München, München, Germany*
[w] *Fachbereich Physik, Bergische Universität Wuppertal, Wuppertal, Germany*
[x] *Panjab University, Chandigarh, India*
[y] *Delhi University, Delhi, India*
[z] *Tata Institute of Fundamental Research, Mumbai, India*
[aa] *University College Dublin, Dublin, Ireland*
[ab] *Korea Detector Laboratory, Korea University, Seoul, Republic of Korea*
[ac] *CINVESTAV, Mexico City, Mexico*
[ad] *Nikhef, Science Park, Amsterdam, The Netherlands*
[ae] *Radboud University Nijmegen, Nijmegen, The Netherlands*
[af] *Joint Institute for Nuclear Research, Dubna, Russia*
[ag] *Institute for Theoretical and Experimental Physics, Moscow, Russia*
[ah] *Moscow State University, Moscow, Russia*
[ai] *Institute for High Energy Physics, Protvino, Russia*
[aj] *Petersburg Nuclear Physics Institute, St. Petersburg, Russia*
[ak] *Institució Catalana de Recerca i Estudis Avançats (ICREA) and Institut de Física d'Altes Energies (IFAE), Barcelona, Spain*
[al] *Uppsala University, Uppsala, Sweden*
[am] *Lancaster University, Lancaster LA1 4YB, United Kingdom*
[an] *Imperial College London, London SW7 2AZ, United Kingdom*
[ao] *The University of Manchester, Manchester M13 9PL, United Kingdom*
[ap] *University of Arizona, Tucson, AZ 85721, USA*
[aq] *University of California Riverside, Riverside, CA 92521, USA*
[ar] *Florida State University, Tallahassee, FL 32306, USA*
[as] *Fermi National Accelerator Laboratory, Batavia, IL 60510, USA*
[at] *University of Illinois at Chicago, Chicago, IL 60607, USA*
[au] *Northern Illinois University, DeKalb, IL 60115, USA*
[av] *Northwestern University, Evanston, IL 60208, USA*
[aw] *Indiana University, Bloomington, IN 47405, USA*
[ax] *Purdue University Calumet, Hammond, IN 46323, USA*
[ay] *University of Notre Dame, Notre Dame, IN 46556, USA*
[az] *Iowa State University, Ames, IA 50011, USA*
[ba] *University of Kansas, Lawrence, KS 66045, USA*

[bb] Kansas State University, Manhattan, KS 66506, USA
[bc] Louisiana Tech University, Ruston, LA 71272, USA
[bd] Northeastern University, Boston, MA 02115, USA
[be] University of Michigan, Ann Arbor, MI 48109, USA
[bf] Michigan State University, East Lansing, MI 48824, USA
[bg] University of Mississippi, University, MS 38677, USA
[bh] University of Nebraska, Lincoln, NE 68588, USA
[bi] Rutgers University, Piscataway, NJ 08855, USA
[bj] Princeton University, Princeton, NJ 08544, USA
[bk] State University of New York, Buffalo, NY 14260, USA
[bl] University of Rochester, Rochester, NY 14627, USA
[bm] State University of New York, Stony Brook, NY 11794, USA
[bn] Brookhaven National Laboratory, Upton, NY 11973, USA
[bo] Langston University, Langston, OK 73050, USA
[bp] University of Oklahoma, Norman, OK 73019, USA
[bq] Oklahoma State University, Stillwater, OK 74078, USA
[br] Brown University, Providence, RI 02912, USA
[bs] University of Texas, Arlington, TX 76019, USA
[bt] Southern Methodist University, Dallas, TX 75275, USA
[bu] Rice University, Houston, TX 77005, USA
[bv] University of Virginia, Charlottesville, VA 22904, USA
[bw] University of Washington, Seattle, WA 98195, USA

ARTICLE INFO

Article history:
Received 2 October 2012
Received in revised form 18 December 2012
Accepted 19 December 2012
Available online 21 December 2012
Editor: M. Doser

ABSTRACT

We present a measurement of the cross section for W boson production in association with at least one b-quark jet in proton–antiproton collisions. The measurement is made using data corresponding to an integrated luminosity of 6.1 fb^{-1} recorded with the D0 detector at the Fermilab Tevatron $p\bar{p}$ Collider at $\sqrt{s} = 1.96$ TeV. We measure an inclusive cross section of $\sigma(W(\to \mu\nu) + b + X) = 1.04 \pm 0.05$ (stat.) $\pm$ 0.12 (syst.) pb and $\sigma(W(\to e\nu) + b + X) = 1.00 \pm 0.04$ (stat.) $\pm$ 0.12 (syst.) pb in the phase space defined by $p_T^{\nu} > 25$ GeV, $p_T^{b\text{-jet}} > 20$ GeV, $|\eta^{b\text{-jet}}| < 1.1$, and a muon (electron) with $p_T^{\ell} > 20$ GeV and $|\eta^{\mu}| < 1.7$ ($|\eta^{e}| < 1.1$ or $1.5 < |\eta^{e}| < 2.5$). The combined result per lepton family is $\sigma(W(\to \ell\nu) + b + X) = 1.05 \pm 0.12$ (stat. + syst.) pb for $|\eta^{\ell}| < 1.7$. The results are in agreement with predictions from next-to-leading order QCD calculations using MCFM, $\sigma(W + b) \cdot \mathcal{B}(W \to \ell\nu) = 1.34^{+0.41}_{-0.34}$ (syst.) pb, and also with predictions from the SHERPA and MADGRAPH Monte Carlo event generators.

The measurement of the production cross section of a W boson in association with a b-quark jet provides a stringent test of quantum chromodynamics (QCD). Processes involving W/Z bosons in association with b quarks are also the largest backgrounds in studies of the standard model (SM) Higgs boson decaying to two b quarks, in measurements of top quark properties in both single and pair production, and in numerous searches for physics beyond the SM. The cross section for the process $p\bar{p} \to W + b + X$ has been calculated with next-to-leading order (NLO) precision [1,2]. Subprocesses at NLO include $q\bar{q} \to Wb\bar{b}$, $q\bar{q} \to Wb\bar{b}g$, and $qg \to Wb\bar{b}q'$. An additional small contribution comes from sea b quarks in the incoming proton or antiproton, $bq \to Wbq'$.

In this Letter we describe a measurement of the cross section for W boson production in association with b-quark jets in $p\bar{p}$ interactions, where a W boson is identified via its electronic or muonic decay modes. A measurement of $W + b$ production cross section with up to two jets at $\sqrt{s} = 1.96$ TeV has been published by the CDF Collaboration [3] and an inclusive measurement has been published by the ATLAS Collaboration [4] at $\sqrt{s} = 7$ TeV. The measured production cross section reported by CDF is $\sigma \cdot \mathcal{B}(W \to \ell\nu) = 2.74 \pm 0.27$ (stat.) $\pm$ 0.42 (syst.) pb ($\ell = e, \mu$), while the theoretical expectation for this quantity based on NLO calculations is 1.22 ± 0.14 (syst.) pb [3]. With the CDF measurement of $W + b$ production exceeding significantly the NLO prediction, while the ATLAS result is in agreement with the expectation, an independent measurement is important to understand the production of W bosons in association with b jets at hadron colliders.

The data used in this analysis were collected between July 2006 and December 2010 using the D0 detector at the Fermilab Tevatron Collider at $\sqrt{s} = 1.96$ TeV, and correspond to an integrated luminosity of 6.1 fb^{-1}. We first briefly describe the main components of the D0 Run II detector [5] relevant to this analysis. The D0 detector has a central tracking system consisting of a silicon microstrip tracker (SMT) [6] and a central fiber tracker (CFT), both located within a 2 T superconducting solenoidal magnet, with designs optimized for tracking and vertexing at pseudorapidities $|\eta| < 3$ and $|\eta| < 2.5$, respectively [7]. A liquid argon and uranium calorimeter has a central section (CC) covering pseudorapidities $|\eta| \lesssim 1.1$, and two end calorimeters (EC) that extend coverage to $|\eta| \approx 4.2$, with all three housed in separate cryostats [8]. An outer muon system, at $|\eta| < 2$, consists of a layer of tracking detectors and scintillation trigger counters in front of 1.8 T toroids, followed by two similar layers after the toroids. Luminosity is measured using plastic scintillator arrays located in front of the EC cryostats. The trigger and data acquisition systems are designed to accommodate the high instantaneous luminosities of Run II.

The $W + b$ candidates are selected by triggering on single lepton or lepton-plus-jet signatures with a three-level trigger system. The

[1] Augustana College, Sioux Falls, SD, USA.
[2] The University of Liverpool, Liverpool, UK.
[3] UPIITA-IPN, Mexico City, Mexico.
[4] DESY, Hamburg, Germany.
[5] SLAC, Menlo Park, CA, USA.
[6] University College London, London, UK.
[7] Centro de Investigacion en Computacion – IPN, Mexico City, Mexico.
[8] ECFM, Universidad Autonoma de Sinaloa, Culiacán, Mexico.
[9] Universidade Estadual Paulista, São Paulo, Brazil.

trigger efficiencies are approximately 70% for the muon channel and 95% for the electron channel. The simulation is corrected for the trigger efficiencies measured in data as described in Ref. [9].

W boson candidates are identified in the $\mu+\nu$ and $e+\nu$ decay channels whereas a small fraction of selected events arises from leptonical decaying tau leptons. Offline event selection requires a reconstructed primary $p\bar{p}$ interaction primary vertex (PV) that has at least three associated tracks and is located within 60 cm of the center of the detector along the beam direction. The vertex selection for $W+b$ events is about 97% efficient as measured in simulations.

Electrons are identified using calorimeter and tracking information. The selection requires exactly one electron with transverse momentum $p_T^e > 20$ GeV identified by an electromagnetic (EM) shower in the central ($|\eta^e| < 1.1$) or endcap ($1.5 < |\eta^e| < 2.5$) calorimeter by comparing the longitudinal and transverse shower profiles to those of simulated electrons. The showers must be spatially isolated from other energetic particles, deposit most of their energy in the EM part of the calorimeter, and pass a likelihood criterion that includes a spatial track match. In the central detector region, an E/p requirement is applied, where E is the energy of the calorimeter cluster and p is the momentum of the track. The transverse momentum measurement of electrons is based on calorimeter energy information [9]. The electron reconstruction efficiency within our restricted phase space is about 98%.

The muon selection requires the candidate to be reconstructed from hits in the muon system and matched to a reconstructed track in the central tracker. The transverse momentum of the muon must exceed $p_T^\mu > 20$ GeV, with $|\eta^\mu| < 1.7$. Muons are required to be spatially isolated from other energetic particles using information from the central tracking detectors and calorimeter [9]. Muons from cosmic rays are rejected by applying a timing criterion on the hits in the scintillator layers and by applying restrictions on the displacement of the muon track with respect to the selected PV. The muon reconstruction efficiency is about 90%.

Candidate $W+$ jets events are then selected by requiring at least one reconstructed jet with $|\eta^{\text{jet}}| < 1.1$ and $p_T^{\text{jet}} > 20$ GeV. Jets are reconstructed from energy deposits in the calorimeter using the iterative midpoint cone algorithm [10] and a cone of radius $\Delta R = 0.5$ in y–φ space [7]. The energies of jets are corrected for detector response, the presence of noise and multiple $p\bar{p}$ interactions, and for energy deposited outside of the jet reconstruction cone [11]. To enrich the sample with W bosons, events are required to have missing transverse energy $\not\!\!E_T > 25$ GeV due to the neutrino escaping detection.

Background processes for this analysis are electroweak $W+$ jets/γ production, Z/γ^* production, $t\bar{t}$ and single top quark production, diboson production, and multijet events with jets misidentified as leptons. The $W+b$ signal and SM background processes are simulated using a combination of PYTHIA v6.409 [12] and ALPGEN v2.3 [13] with PYTHIA providing parton showering and hadronization. We use PYTHIA Tune A with CTEQ6L1 [14] parton distribution functions (PDFs) and perform a detailed GEANT-based [15] simulation of the D0 detector. The $V+$ jets ($V = W/Z$) processes are normalized to the inclusive W and Z-boson cross sections calculated at NNLO [16]. The Z-boson p_T distribution is modeled to match the distribution observed in data [17], taking into account the dependence on the number of reconstructed jets. To reproduce the W-boson p_T distribution in simulated events, the product of the measured Z-boson p_T spectrum and the ratio of W to Z-boson p_T distributions at NLO is used as correction [17,18]. NLO + NNLL (next-to-next-to-leading log) calculations are used to normalize $t\bar{t}$ production [19], while single top quark production is normalized to NNLO [20]. The NLO WW, WZ, and ZZ production cross section values are obtained with MCFM program [21]. For the $W+$ heavy-flavor jet (b or c quark) events, the ratio of the ALPGEN prediction to the NLO prediction for $W+b\bar{b}$ and $W+c\bar{c}$ is obtained from MCFM [21] and applied as a correction factor. The simulation is also corrected for the trigger efficiencies measured in data.

Instrumental backgrounds and those from semileptonic decays of hadrons, referred to as "multijet" background, are estimated from data using the "matrix method" as described in Ref. [9]. The instrumental background is important for the electron channel, where a jet with a high electromagnetic fraction can pass electron identification criteria, or a photon can be misidentified as an electron. In the muon channel, the multijet background is less significant and arises mainly from the semileptonic decay of heavy quarks in which the muon satisfies the isolation requirements. We require that the W boson candidates have a transverse mass M_T [22] satisfying $40\ \text{GeV} + \frac{1}{2}\not\!\!E_T < M_T < 120$ GeV to suppress multijet background and mis-reconstructed events. The average efficiency determined in simulation for a $W+b$ signal to pass these requirements is about 82%.

Identification of b jets is crucial for this measurement. Once the inclusive $W+$ jets sample is defined, the jets considered for b tagging are subject to a requirement called taggability. This requirement is imposed to decouple the performance of the b-jet identification from detector effects. For a jet to be taggable, it must contain at least two tracks with at least one hit in the SMT, $p_T > 1$ GeV for the highest-p_T track and $p_T > 0.5$ GeV for the next-to-highest p_T track. The efficiency for a jet to be taggable is about 90% in the selected phase space.

The D0 b-tagging algorithm for identifying heavy flavor jets is based on a combination of variables sensitive to the presence secondary vertices (SV) or tracks displaced from the PV. This analysis uses an updated b tagger utilizing a multivariate analysis (MVA) [23,24] that provides improved performance over the previous neural network based algorithm [25]. The most sensitive input variables to the MVA are the number of reconstructed secondary vertices in the jet, the invariant mass of charged particles associated with the SV (M_{SV}), the number of tracks used to reconstruct the SV, the two-dimensional decay length significance of the SV in the plane transverse to the beam, a weighted combination of the tracks' transverse impact parameter significances, and the probability that the tracks from the jet originate from the PV, which is referred to as the jet lifetime probability (JLIP). The MVA provides a continuous output value that tends towards one for b jets and zero for non-b jets. Events are considered in which at least one jet passes a tight MVA requirement corresponding to an efficiency of $\approx 50\%$ for b jets. The likelihood for a light jet (u, d, s quarks and gluons) to be misidentified for the corresponding MVA selection is about 1%. Simulated events are corrected to have the same efficiencies for taggability and b-tagging requirements as found in data. These corrections are derived in a flavor dependent manner [25], using independent QCD enriched data samples and simulated events with enriched light and heavy jet contributions. Jets containing b quarks have a different energy response and receive an additional energy correction of about 6% as determined from simulation. Fig. 1 shows the transverse mass of the candidate events before and after applying b-jet identification.

In addition to the MVA output, we deduce further information by combining the M_{SV} and JLIP variables [24]. M_{SV} provides good discrimination between b, c, and light quark jets due to their different masses. The two variables together take into account the kinematics of the event and, in order to further improve the separation power, they are combined in a single variable $\mathcal{D}_{\text{MJL}} = \frac{1}{2}(M_{\text{SV}}/(5\ \text{GeV}) - \ln(\text{JLIP})/20)$ [26]. A loose criterion for an event to pass at least $\mathcal{D}_{\text{MJL}} > 0.1$ is applied to remove poorly

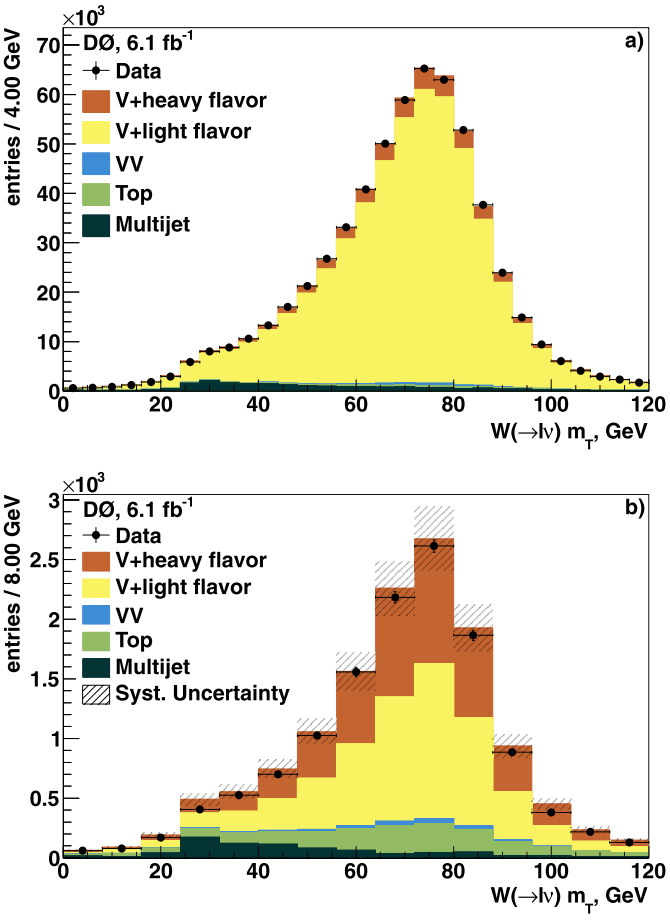

Fig. 1. (Color online.) Transverse mass of the $\ell\nu$ system (a) before and (b) after b-jet identification. The data are shown by black markers, simulated background processes are shown by filled histograms. The data uncertainties are statistical only. An estimate of the systematic uncertainty on the simulated background processes is shown by the shaded bands.

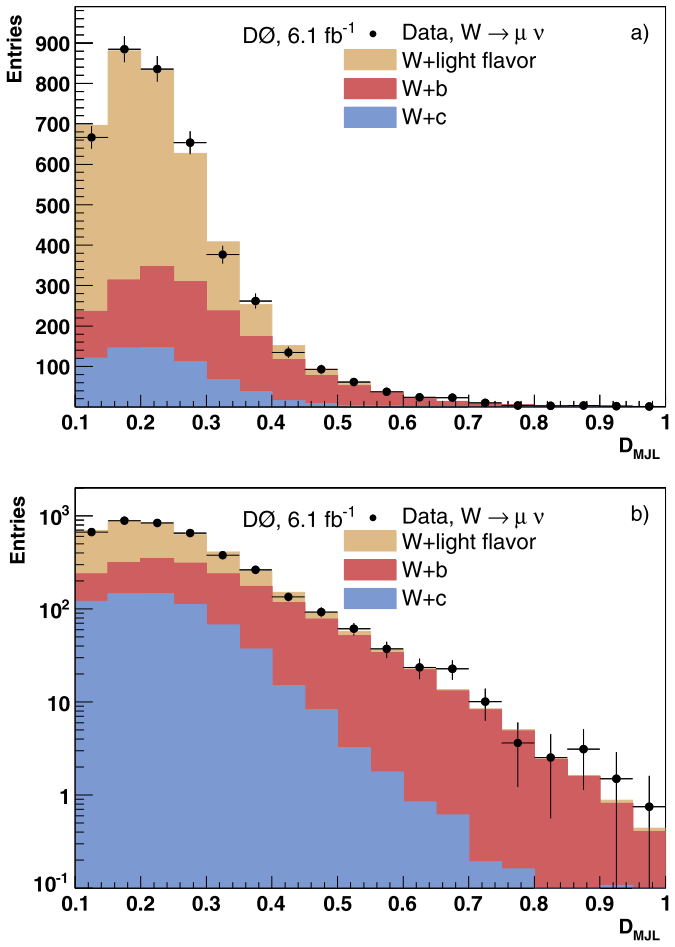

Fig. 2. (Color online.) Contributions of the various jet flavors normalized to the measured cross section obtained from a fit in the $W \to \mu\nu$ channel on both (a) linear and (b) logarithmic scales. The various W + jets processes are shown as filled histograms and data, after the subtraction of contributions from Drell–Yan, diboson, and top quark production, are represented with black markers. The uncertainties include both statistical and systematic contributions.

Table 1
Numbers of events for data and contributing processes before and after applying b-jet identification. Additional requirements are applied to the b-tagged sample as described in the text. Uncertainties include statistical and systematic contributions. The contribution of Z + jets events to the V + jets samples is $\approx 5\%$ for heavy and light flavor jets before and after b-tagging.

Process	No b-tag	b-tag
V + heavy flavor	$41\,093 \pm 8924$	5068 ± 1124
V + light flavor	$516\,661 \pm 56\,734$	5718 ± 678
Diboson	4728 ± 519	222 ± 26
Top	5431 ± 536	1602 ± 181
Multijet	$20\,527 \pm 4458$	794 ± 180
Expected events	$588\,440 \pm 57\,610$	$13\,405 \pm 1338$
Data	586 289	12 793

Table 2
Estimated numbers of W + jet events from fitting the flavor-specific processes, along with the data after subtracting Z + jets, single top quark, $t\bar{t}$, and diboson background processes. l.f. stands for light flavor jets. Uncertainties include statistical and systematic contributions.

Process	$W \to \mu\nu$		$W \to e\nu$	
	Events	Fraction	Events	Fraction
$W + b$	1306 ± 166	0.32 ± 0.04	1676 ± 212	0.27 ± 0.03
$W + c$	664 ± 97	0.16 ± 0.02	1096 ± 159	0.18 ± 0.03
W + l.f.	2152 ± 265	0.52 ± 0.07	3479 ± 425	0.56 ± 0.07
Data–Bkgd	4127 ± 150		6255 ± 168	

reconstructed events. The efficiency for signal events to pass this selection is about 97%.

The numbers of expected and observed events before and after applying the b-jet identification in data and simulation are listed in Table 1. The b-tagging column includes the selection requirement on $\mathcal{D}_{\mathrm{MJL}}$.

We measure the fraction of $W + b + X$ events in the final selected sample by performing a binned maximum likelihood fit to the observed data distribution of the $\mathcal{D}_{\mathrm{MJL}}$ discriminant in our sample shown in Fig. 2. The templates for W + light flavor, $W + b$, and $W + c$ jets shown in Fig. 2 are taken from the simulation. Expected contributions from Z + jets, single top quark, $t\bar{t}$, diboson, and multijet production are subtracted from the data. After performing the fits, we obtain the number of events with different jet flavors listed in Table 2.

We quote our result as a cross section in a restricted phase space: at least one b-jet with $p_T^{b\text{-jet}} > 20$ GeV, $|\eta^{b\text{-jet}}| < 1.1$ and a muon with $p_T^{\mu} > 20$ GeV and $|\eta^{\mu}| < 1.7$ or an electron with $p_T^{e} > 20$ GeV and $|\eta^{e}| < 1.1$ or $1.5 < |\eta^{e}| < 2.5$. For the neutrino momentum we require $p_T^{\nu} > 25$ GeV. Corrections for trigger, lepton, jet and b-tagging requirements are applied as function of absolute pseudorapidity and momentum [9]. Acceptance, migration

in and out of the restricted phase space, and selection efficiencies have been studied using the simulation and corrected. The measured cross sections are therefore presented at the particle level.

The effects of systematic uncertainties are determined through nuisance parameters that are assigned Gaussian probability distributions. Each nuisance parameter can affect rates of the predicted signal and background in the $\mathcal{D}_{\mathrm{MJL}}$ distribution. Systematic uncertainties such as predicted SM cross sections, b-tagging efficiencies, and energy calibration affect the predictions of signal and background and are treated as fully correlated across channels. Uncertainties for lepton identification and triggering are not correlated. The systematic uncertainties are dominated by effects related to the measurement of jets. The contributions from jet energy resolution, jet modeling, and detector effects are about 2.5%, 3%, and 4%, respectively. Uncertainties on b-jet identification are determined in data and simulations by using b-jet-enriched samples and are about 2%–5% per jet. The uncertainties due to lepton identification are about 2%. The integrated luminosity is known to a precision of 6.1% [27]. The uncertainty of the template fit is estimated by varying the normalization and shape from the data corrections of the W boson processes and the fit parameters (about 6%). By summing the uncertainties in quadrature we obtain a final total systematic uncertainty on the cross section measurements of approximately 12%.

The cross section times branching fraction is calculated by dividing the number of signal events measured by integrated luminosity ($\mathcal{L}$), acceptance ($\mathcal{A}$), and efficiencies (ϵ) of the selection requirements:

$$\sigma(W+b)\cdot\mathcal{B}(W\to\ell\nu)=\frac{N_{W+b}}{\mathcal{L}\cdot\mathcal{A}\cdot\epsilon}, \tag{1}$$

where ϵ is given by the product of the trigger, object reconstruction, and selection efficiencies.

We first present results separately for the muon channel and electron channel because they are performed in slightly different requirements on the phase space of the lepton and then combine using a common phase space. We measure from the cross section in the muon channel where $W\to\mu\nu$ in a visible phase space defined by $p_T^{\mu}>20$ GeV, $|\eta^{\mu}|<1.7$ with at least one b-jet limited to $p_T^{b\text{-jet}}>20$ GeV and $|\eta^{b\text{-jet}}|<1.1$ as,

$$\sigma(W+b)\cdot\mathcal{B}(W\to\mu\nu) = 1.04\pm0.05\,(\text{stat.})\pm0.12\,(\text{syst.})\ \text{pb}. \tag{2}$$

We perform an NLO QCD prediction using MCFM v6.1, based on CTEQ6M PDF [14] and a central scale of M_W+2m_b, where $m_b=4.7$ GeV is the mass of the b quark. Uncertainties are estimated by varying renormalization and factorization scales by a factor of two in each direction, varying m_b between 4.2 and 5 GeV, and by using an alternative PDF set. The MCFM calculation predicts $\sigma(W+b)\cdot\mathcal{B}(W\to\mu\nu)=1.34^{+0.40}_{-0.33}\,(\text{scale})\pm0.06\,(\text{PDF})^{+0.09}_{-0.05}\,(m_b)$ pb. Predictions obtained using SHERPA v1.4 and CTEQ6.6 PDFs [14] lead to a value 1.21 ± 0.03 (stat.) pb. Using MADGRAPH5 [28] with CTEQ6L1 PDFs, we obtain 1.52 ± 0.02 (stat.) pb. Uncertainties for scale variations, PDFs, and the b-quark mass are on the order of about 30%.

In the electron channel, we measure the cross section times branching fraction by selecting $p_T^{e}>20$ GeV, $|\eta^{e}|<1.1$ or $1.5<|\eta^{e}|<2.5$, at least one b-jet as above and obtain

$$\sigma(W+b)\cdot\mathcal{B}(W\to e\nu) = 1.00\pm0.04\,(\text{stat.})\pm0.12\,(\text{syst.})\ \text{pb}. \tag{3}$$

The MCFM calculated cross section for this channel is $\sigma(W+b)\cdot\mathcal{B}(W\to e\nu)=1.28^{+0.40}_{-0.33}\ (\text{scale})\pm0.06\ (\text{PDF})^{+0.09}_{-0.05}\ (m_b)$ pb. The SHERPA prediction is 1.08 ± 0.03 (stat.) pb, while the MADGRAPH5 prediction is 1.44 ± 0.02 (stat.) pb. The combined systematic effect scale, PDF and m_b variations is also around 30%.

Using the MCFM prediction we extrapolate the measurement in the electron final state to the same selection requirements as the muon final state to allow for a consistent combination. Combining the results in $W\to\mu\nu$ and $W\to e\nu$ decays we obtain

$$\sigma(W+b)\cdot\mathcal{B}(W\to\ell\nu) = 1.05\pm0.03\,(\text{stat.})\pm0.12\,(\text{syst.})\ \text{pb}. \tag{4}$$

The small experimental uncertainty should allow to further constrain theoretical predictions. In summary, we have performed a measurement of the inclusive cross section for W boson production in association with at least one b-jet at $\sqrt{s}=1.96$ TeV, considering final states with $W\to\mu\nu$ ($W\to e\nu$) events in a restricted phase space of $p_T^{\ell}>20$ GeV, $|\eta^{\mu}|<1.7$ ($|\eta^{e}|<1.1$ or $1.5<|\eta^{e}|<2.5$), with b jets limited to $p_T^{b\text{-jet}}>20$ GeV and $|\eta^{b\text{-jet}}|<1.1$. The measured cross sections agree within uncertainties with NLO QCD calculations and predictions obtained using the SHERPA and MADGRAPH generators.

Acknowledgements

We thank the staffs at Fermilab and collaborating institutions, and acknowledge support from the DOE and NSF (USA); CEA and CNRS/IN2P3 (France); MON, NRC KI and RFBR (Russia); CNPq, FAPERJ, FAPESP and FUNDUNESP (Brazil); DAE and DST (India); Colciencias (Colombia); CONACyT (Mexico); NRF (Korea); FOM (The Netherlands); STFC and the Royal Society (United Kingdom); MSMT and GACR (Czech Republic); BMBF and DFG (Germany); SFI (Ireland); The Swedish Research Council (Sweden); and CAS and CNSF (China). Special thanks as well to John Campbell for his support with MCFM and Patrick Fox with MADGRAPH.

References

[1] J. Campbell, R.K. Ellis, F. Maltoni, S. Willenbrock, Phys. Rev. D 75 (2007) 054015.
[2] J. Campbell, et al., Phys. Rev. D 79 (2009) 034023.
[3] T. Aaltonen, et al., CDF Collaboration, Phys. Rev. Lett. 104 (2010) 131801.
[4] G. Aad, et al., ATLAS Collaboration, Phys. Lett. B 707 (2012) 418.
[5] V.M. Abazov, et al., D0 Collaboration, Nucl. Instrum. Methods Phys. Res. A 565 (2006) 463.
[6] R. Angstadt, et al., Nucl. Instrum. Methods Phys. Res. A 622 (2010) 298.
[7] We use a standard right-handed coordinate system. The nominal collision point is the center of the detector with coordinate $(0,0,0)$. The direction of the proton beam is the positive $+z$ axis. The $+x$ axis is horizontal, pointing away from the center of the Tevatron ring. The $+y$ axis points vertically upwards. The polar angle, θ, is defined such that $\theta=0$ is the $+z$ direction. The rapidity is defined as $y=-\ln[(E+p_Z)/(E-p_Z)]$, where E is the energy and p_Z is the momentum component along the proton beam direction. Pseudorapidity is defined as $\eta=-\ln(\tan\frac{\theta}{2})$. φ is defined as the azimuthal angle in the plane transverse to the proton beam direction.
[8] S. Abachi, et al., D0 Collaboration, Nucl. Instrum. Methods Phys. Res. A 324 (1993) 53.
[9] V.M. Abazov, et al., D0 Collaboration, Phys. Rev. D. 86 (2012) 032005.
[10] G.C. Blazey, et al., FERMILAB-CONF-00-092-E, 2000.
[11] V.M. Abazov, et al., D0 Collaboration, Phys. Rev. D Phys. 85 (2012) 052006.
[12] T. Sjöstrand, et al., Comput. Phys. Commun. 135 (2001) 238.
[13] M. Mangano, et al., J. High Energy Phys. 0307 (2003) 001.
[14] J. Pumplin, et al., J. High Energy Phys. 02012 (2002) 0207.
[15] S. Agostinelli, et al., Nucl. Instrum. Methods Phys. Res. A 506 (2003) 250.
[16] R. Hamberg, W.L. van Neerven, T. Matsuura, Nucl. Phys. B 644 (2002) 403.
[17] V.M. Abazov, et al., D0 Collaboration, Phys. Lett. B 669 (2008) 278.
[18] V.M. Abazov, et al., D0 Collaboration, Phys. Lett. B 705 (2011) 200.
[19] S. Moch, P. Uwer, Phys. Rev. D 78 (2008) 034003.
[20] N. Kidonakis, Phys. Rev. D 74 (2006) 114012.
[21] J. Campell, R.K. Ellis, Nucl. Phys. Proc. Suppl. 205 (2010) 10.
[22] Since the longitudinal component of the momentum of the neutrinos is not measured, the measured properties of the W boson candidates are limited to their transverse energy and transverse mass, defined as

$M_T = \sqrt{(\not{p}_T + p_T^\ell)^2 - (\not{p}_x + p_x^\ell)^2 - (\not{p}_y + p_y^\ell)^2}$ where $\not{p}_T$ is the magnitude of the missing transverse energy vector, p_T^ℓ is the transverse momentum of the lepton and p_x^ℓ and p_y^ℓ ($\not{p}_x$ and $\not{p}_y$) are the magnitude of the x and y components of the lepton's momentum (missing transverse energy) respectively.

[23] A. Hoecker, PoS ACAT, 2007, 040, CERN–OPEN-2007-007.

[24] V.M. Abazov, et al., D0 Collaboration, Phys. Lett. B 714 (2012) 32.

[25] V.M. Abazov, et al., D0 Collaboration, Nucl. Instrum. Meth. A 620 (2010) 490.

[26] V.M. Abazov, et al., D0 Collaboration, Phys. Rev. D 83 (2011) 031105.

[27] T. Andeen, et al., FERMILAB-TM-2365, 2007.

[28] J. Alwall, et al., J. High Energy Phys. 1106 (2011) 128.